MAGNETOTELLURIC AND GEOMAGNETIC DEPTH SOUNDING METHODS COMPARED IN SOUTHERN AUSTRALIA.

F.E.M. Lilley*, D.I. Gough** and H.Y. Tammemagi*

*Department of Geophysics and Geochemistry,
Australian National University, Canberra

**Institute of Earth and Planetary Physics,
University of Alberta, Edmonton, Canada.

for submission to Nature 10 August 1972.

The electrical conductivity structure of the earth may be explored by measuring electric and magnetic field variations which are induced by magnetic storms. At any point on the surface of the earth five time-varying elements may be observed: the northward (X) eastward (Y) and vertically down (Z) magnetic field components, and the northward (A) and eastward (B) surface electric field components. In the magnetotelluric (M-T) method only the horizontal components X,Y,A, and B are observed, whereas in the geomagnetic depth sounding (GDS) method only the magnetic components X,Y, and Z are observed. As these methods are equivalent only under certain special circumstances, there is usually an advantage in observing all five elements.

This paper reports some observations made of all five elements in southern Australia, when, for the first time, telluric recording equipment was operated in conjunction with a magnetic variometer array. The array experiment was that reported by Gough et al.[1], for which twenty-five magnetic variometers were in operation simultaneously at the sites shown in Figure 1. Three sets of telluric recording equipment were moved across the array[2] during the experiment, to occupy nine of the magnetometer sites, as also marked on Figure 1. An example of the magnetic variations data recorded at all stations is shown in Figure 2; and an example of simultaneous magnetic and telluric data is shown in Figure 3. It has been possible to display combinations of the data in novel ways, for example, superimposed horizontal polarization ellipses for all magnetic stations and three telluric stations are shown in Figure 4.

Interpretation of the data has been carried out for the Pimba-Yelta line, (PIM-YEL) using both M-T and G D S methods, and the results of each are now compared.

The M-T apparent resistivity curves, calculated from impedance tensors rotated into principal axes, are shown in Figure 5; in each case, the direction of maximum apparent resistivity is close to north-south, and that of minimum resistivity close to east-west. The most notable feature is the very low apparent resistivity recorded at Waukaringa (WAK) and Mulyungarie (MLY). On the assumption that the line Pimba-Yelta lies across a two-dimensional conductivity inhomogeneity, these data have been interpreted[2] in terms of the model shown under the curves in Figure 5.

To introduce the G D S interpretation, some magnetic variation maps are shown in Figure 6, for circular polarization of the horizontal field. The strongest feature is the phase change of approximately half a cycle in the Z-phase map, which has been emphasized by the heavy dotted line. This feature is explained by a good conductor directly below the region of the phase change. Simple models would predict a zero of amplitude along this line, although the station spacing has evidently been too coarse to detect this null. However, it should be noted that the non-zero amplitude contours crossing the dotted phase line may be quite erroneous.

The electrical conductivity below the PIM-YEL traverse has been modelled by numerical techniques[3,4] for two-dimensional structures; Figure 7 shows three models, with superimposed phase and amplitude data for an eastwards polarized

field, for period T = 34 min. It is seen that the theoretical Z phase curves for all three models fit the measured phases very well. The amplitude data offers a means of discrimination between the models, and Figure 7 shows that the theoretical Z-amplitude response discriminates against Model 1. A preliminary examination of data at both longer and shorter periods indicates that the conductor is quite shallow and may thus be like Model 3, tapering off to either side.

Both the M-T and G D S models of the structure under the PIM-YEL traverse indicate that a good conductor exists beneath the WAK-MLY section. Because of the separation (or anisotropy) of the measured apparent resistivity curves, the final M-T model of Figure 5 was determined within relatively wide limits. However, no model could be found whose theoretical response exactly satisfied all the M-T curves and all the G D S data. In Figure 8 is shown one possible compromise model. As it fits neither data set exactly, it must indicate some departure of the actual conditions from the original simplifying assumptions. It is a distinct possibility that the mechanisms which caused the anisotropy of the apparent resistivity curves have distorted them slightly, particularly at Waukaringa and Mulyungarie. On the other hand, it is also possible that the magnetometer array was too sparsely located to detect the narrow Z-amplitude peaks of the M-T models of Figure 5 and 8, (which have sharp Z- amplitude responses like that of Model 1 in Figure 7).

The present exercise has demonstrated the M-T and G D S methods to be quite complementary to each other. The magnetotelluric method has acted as a calibrator, yielding important information on the absolute resistivity values involved, as well as locating the anomaly between Partacoona (PAR) and Hazelvale(HAZ) and showing it to be situated in the crust.

The magnetometer array has acted as a delineator, locating the anomaly and tracing its path. In addition it has yielded valuable information concerning the anisotropy of the observed apparent resistivities shown in Figure 5. This anisotropy is not accounted for by any of the models of Figures 5,7 and 8. To be explained by induction, it would require a very strong conductivity contrast striking east-west and lying either to the north or south of the magnetotelluric traverse. This possibility is precluded, however, by the absence from the magnetometer data of the anomalous Z pattern which should also then be observed. The M-T anisotropy is thus suspected as having been caused locally by conduction in small-scale inhomogeneities rather than by induction on a regional scale. Accurate interpretation of such anisotropy may well be impossible.

It remains to discuss the geological significance of the line of good conductor. This may be buried sediment, perhaps a strongly downwarped flank of the Adelaide Geosyncline. Alternatively it may indicate a shear-zone associated with the continental tectonics of Australia[5], though the fact that it lies along the eastern boundary of the seismic activity is very curious. Figure 9 summarizes this evidence. It will be of some interest to ultimately search for this conductor both to the north and south of the present array.

References

1. Gough, D.I., Lilley, F.E.M. and McElhinny, M.W., Nature, submitted (1972).
2. Tammemagi, H.Y., and Lilley, F.E.M., Geophysics, submitted (1972).
3. Jones, F.W. and Pascoe, L.J., Geophys. J., 24, 3 (1971).
4. Pascoe, L.J. and Jones, F.W., Geophys. J., 27, 179 (1972).
5. Cleary, J.R., and Simpson, D.W., Nature, 230, 239 (1971).
6. Stewart, I.C.F. and Mount, T.J., J. Geol. Soc. Austral., in press (1972).

Figure Captions

Fig. 1. Map of observing sites in southern Australia.

Fig. 2. Magnetic variometer profiles for 16 October 1970.

Fig. 3. Simultaneous telluric (A,B) and magnetic (H,D) records from three central stations. A and H are measured in the direction of magnetic north, B and D in the direction of magnetic east. For layered structure, A should correlate with D, and B with H. Note the very weak telluric signals from station WAK.

Fig. 4. Ellipses of horizontal polarization; telluric ellipses (dotted) for PIM, PAR and WAK are superimposed upon the magnetic ellipses (solid lines) for all stations. Period T = 43.6 min.

Fig. 5. M-T apparent resistivity data and proposed model. The data points, plotted with error bars, are for maximum and minimum directions of resistivity. The curves show the theoretical response of the model drawn below. Solid curves are for electric field parallel to strike, magnetic field across strike; dashed curves are for vice-versa. If no dashed curve is shown, it lies coincident with the solid curve.

Fig. 6. Contoured maps of amplitude and phase values obtained by Fourier transforming magnetograms; for a circular polarization, period T = 25 min.

Fig. 7. The responses of three models investigated while modelling the G D S data. All models fit the phase data well; Model 3 is regarded as fitting the amplitude data reasonably well. The models are of resistivity 10 ohm-m in a background resistivity of 1000 ohm-m.

Fig. 8. Compromise model for M-T and G D S data combined.

Fig. 9. Axis of the Z-reversal, (i.e. phase change of half a cycle), plotted against the seismicity of the Adelaide Geosyncline region[6].

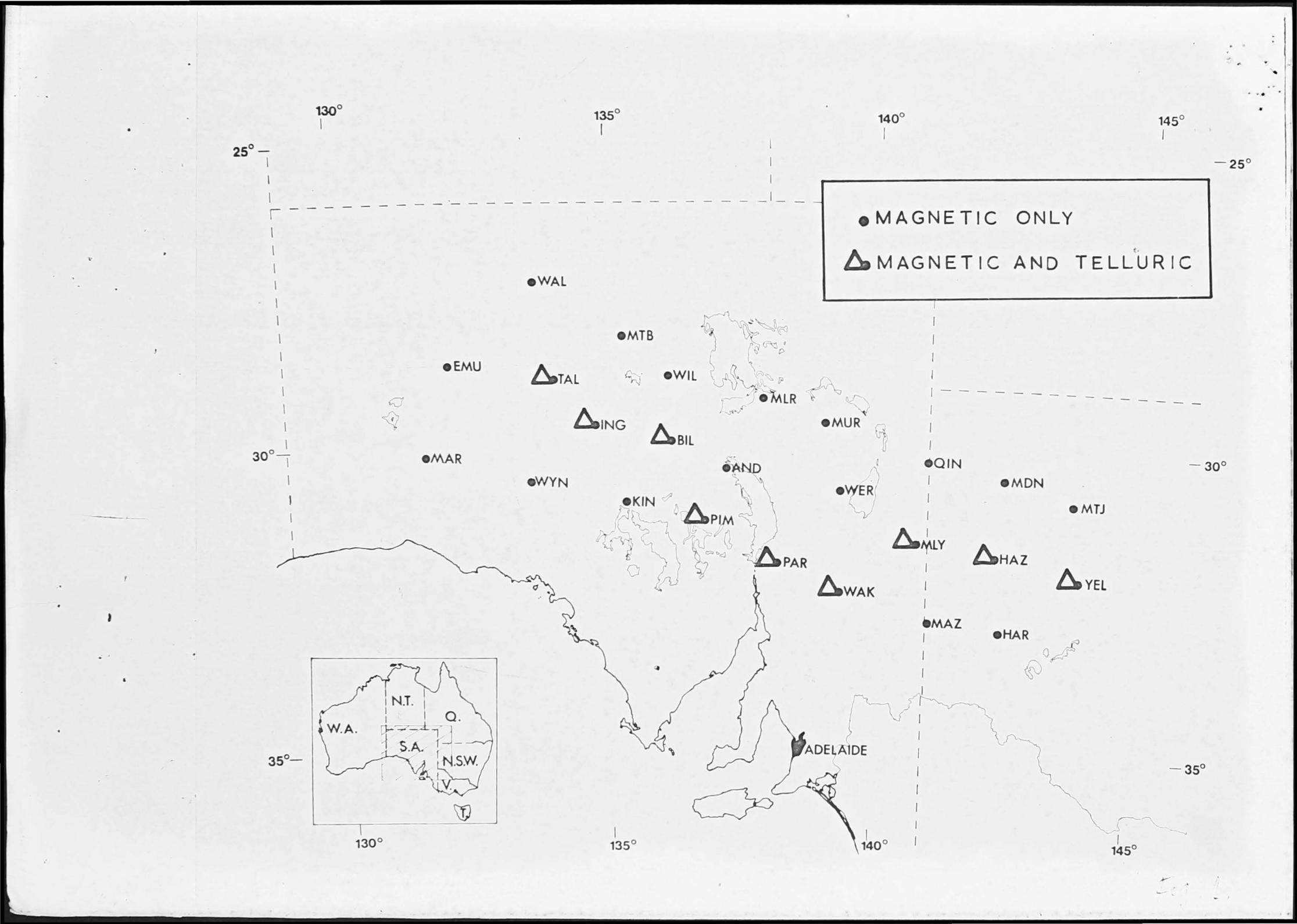
130°
135°
140°
145°
25°
30°
35°
MAGNETIC ONLY
MAGNETIC AND TELLURIC
WAL
MTB
EMU
TAL
WIL
MLR
ING
MUR
BIL
MAR
AND
QIN
MDN
WYN
WER
KIN
MTJ
PIM
MLY
HAZ
PAR
YEL
WAK
MAZ
HAR
ADELAIDE
N.T.
Q.
W.A.
S.A.
N.S.W.
V.
T.

16 OCTOBER 1970

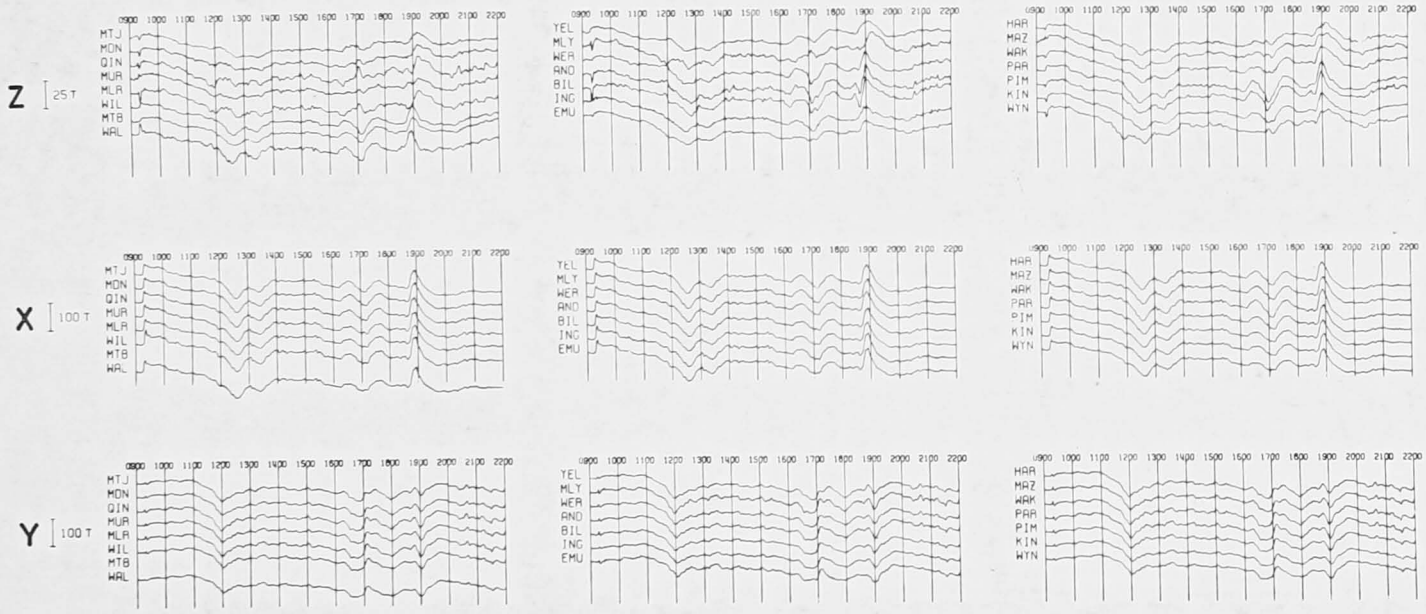

Fig. 2

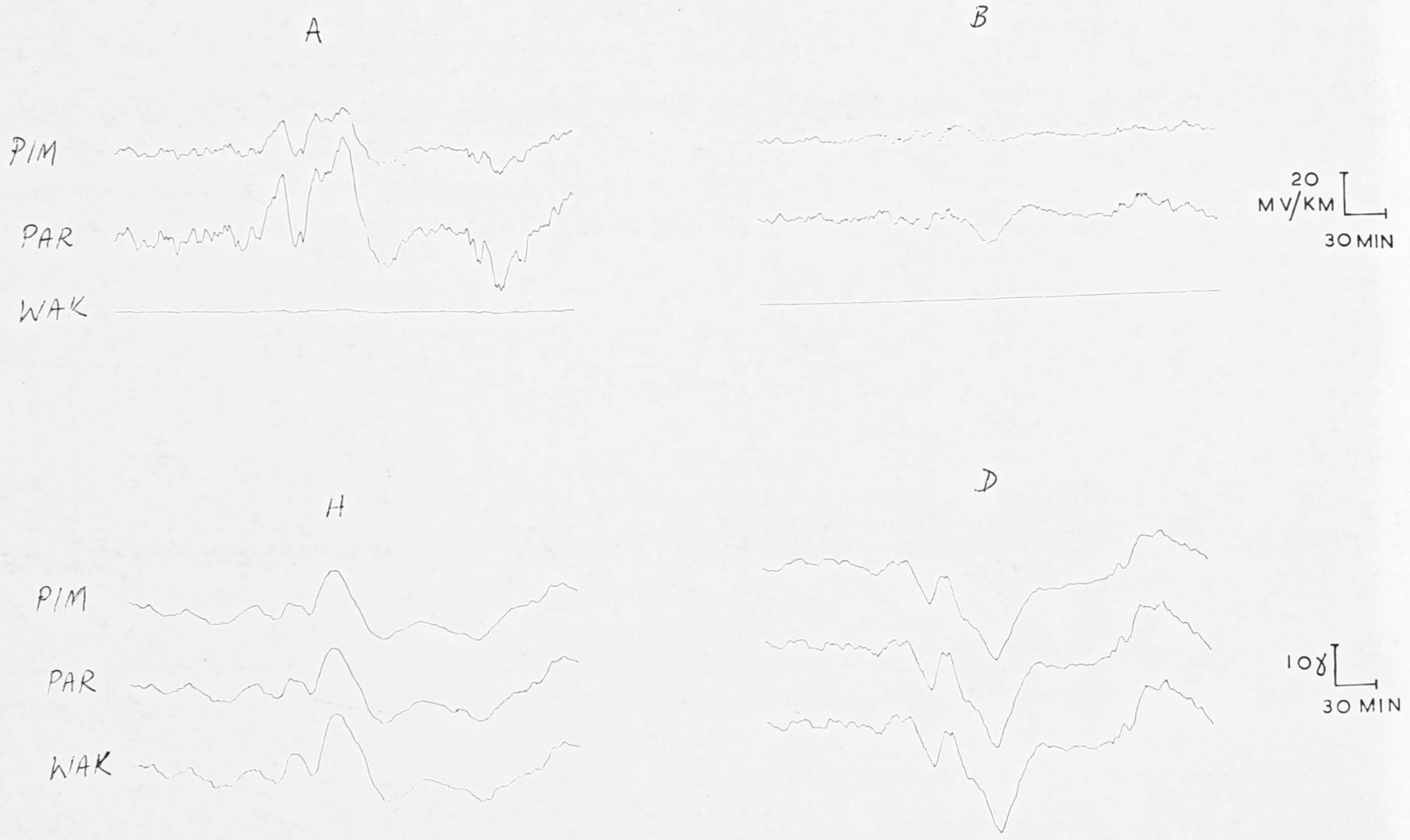
A
PIM
PAR
WAK
B
20
MV/KM
30 MIN
H
PIM
PAR
WAK
D
10γ
30 MIN

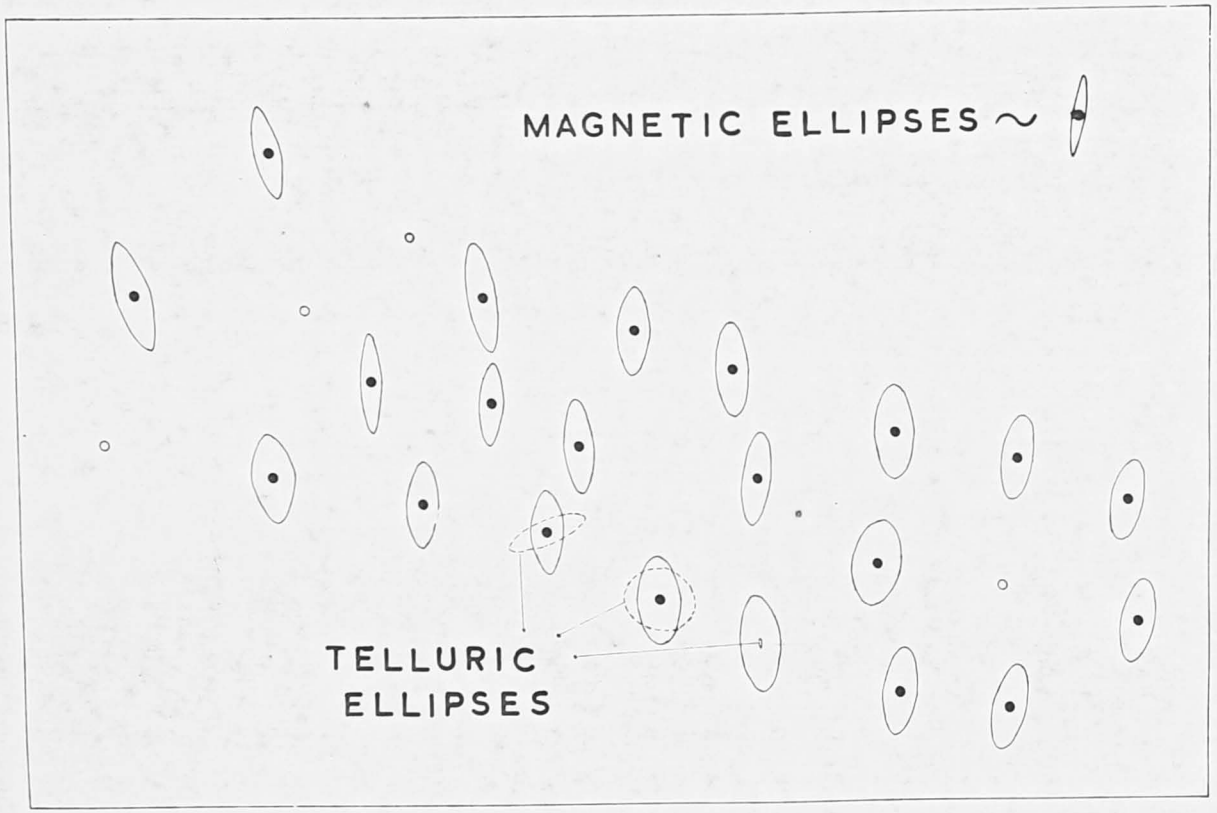

Fig. 1

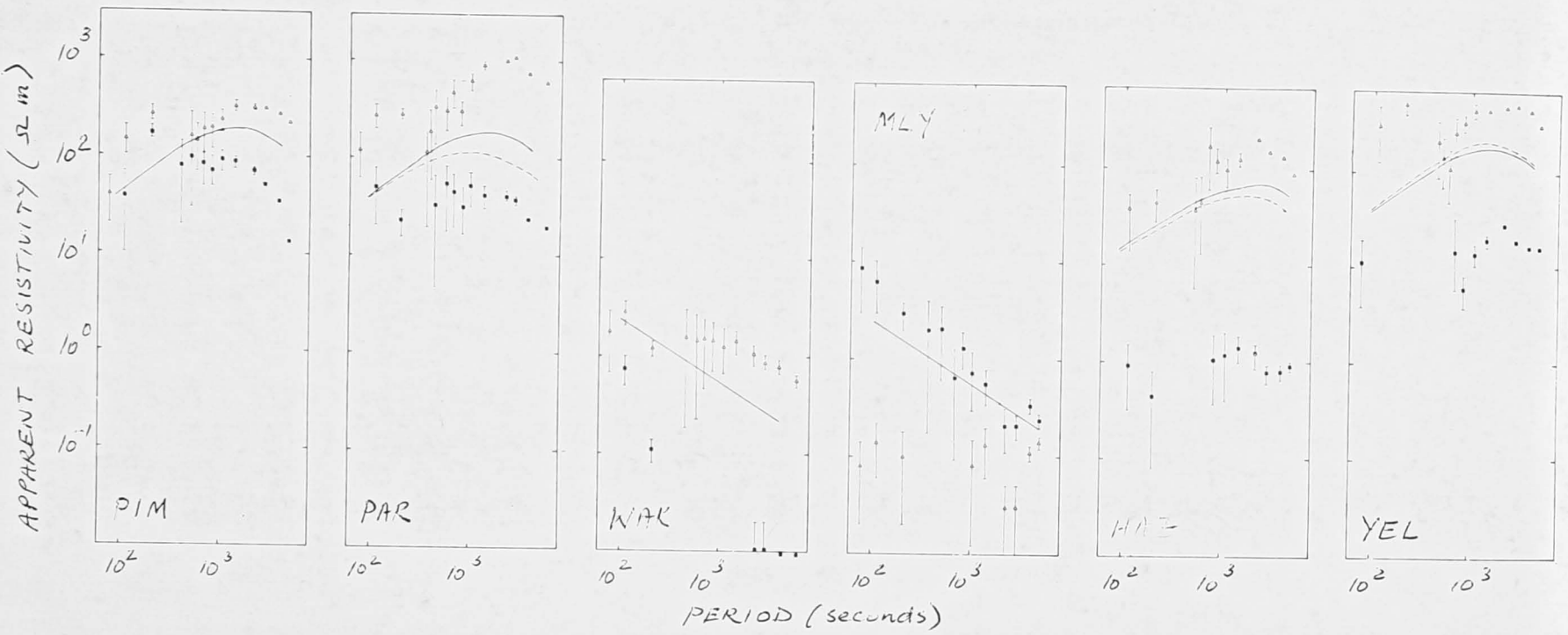
APPARENT RESISTIVITY (Ω m)
10^3
10^2
10^1
10^0
10^{-1}
DIM
PAR
WIK
MLY
HAI
YEL
10^2
10^3
PERIOD (seconds)

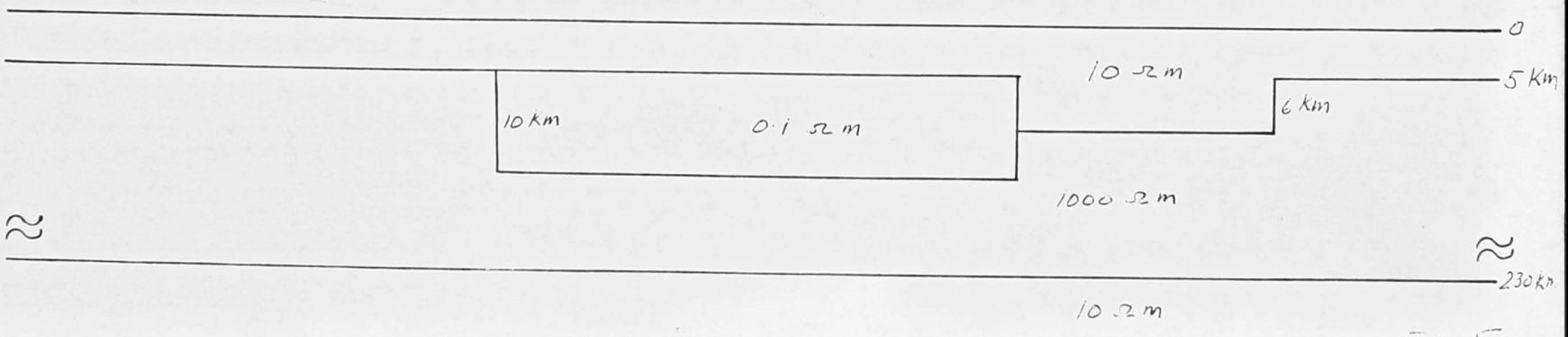
0
10 Ω m
5 km
6 km
10 km
0.1 Ω m
1000 Ω m
230 km
10 Ω m

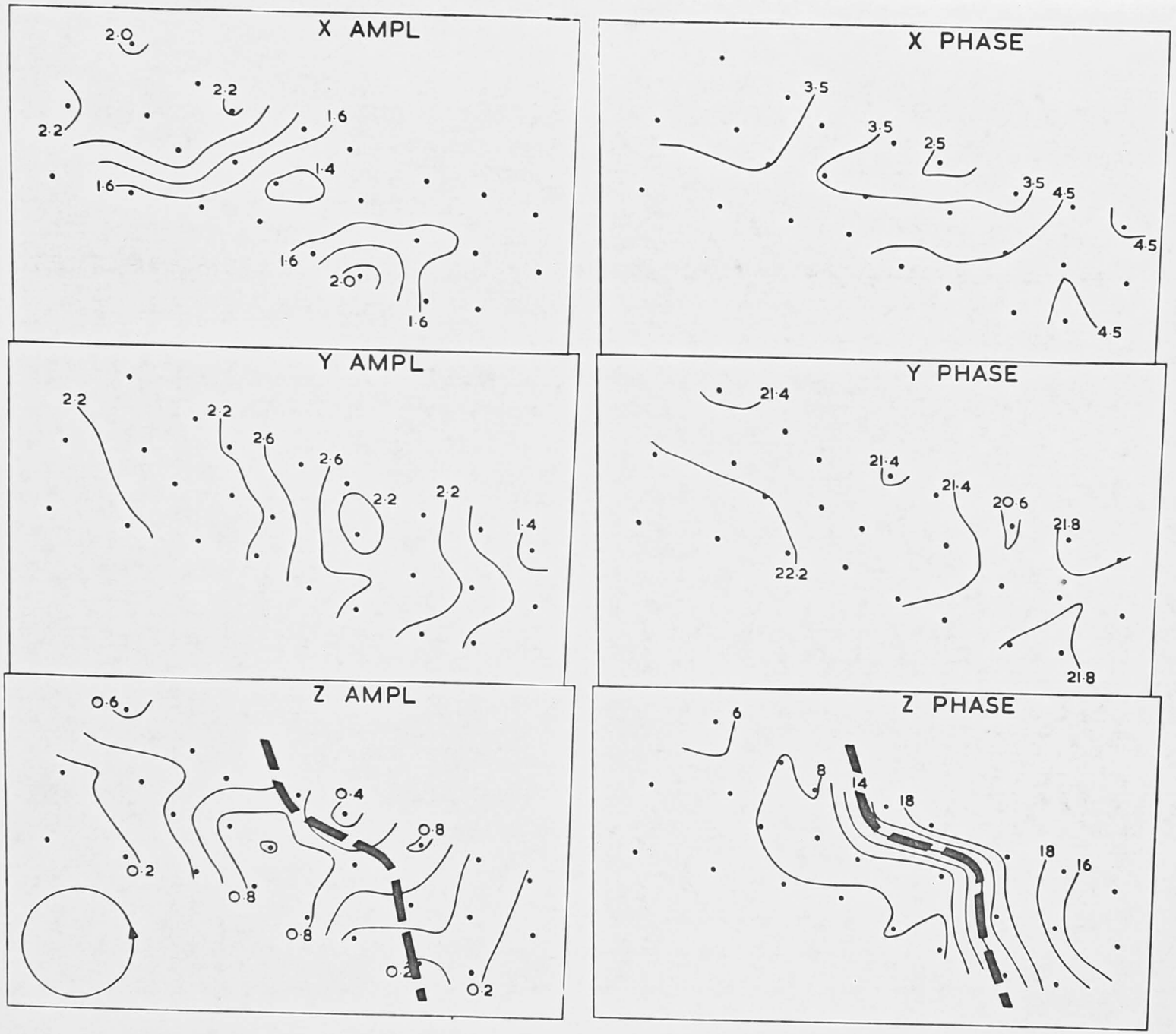
X AMPL
2·0
2·2
2·2
1·6
1·4
1·6
1·6
2·0
1·6
X PHASE
3·5
3·5
2·5
3·5
4·5
4·5
4·5
Y AMPL
2·2
2·2
2·6
2·6
2·2
2·2
1·4
Y PHASE
21·4
21·4
21·4
20·6
21·8
22·2
21·8
Z AMPL
0·6
0·4
0·8
0·2
0·8
0·8
0·2
0·2
Z PHASE
6
8
14
18
18
16

Y - PHASE

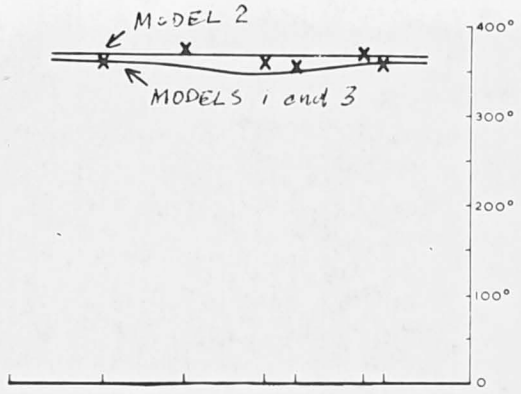

Z - PHASE

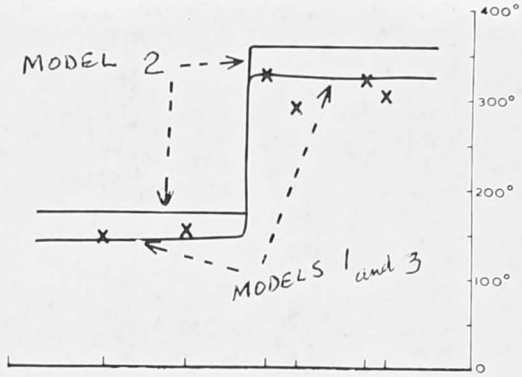

Y - AMPLITUDE

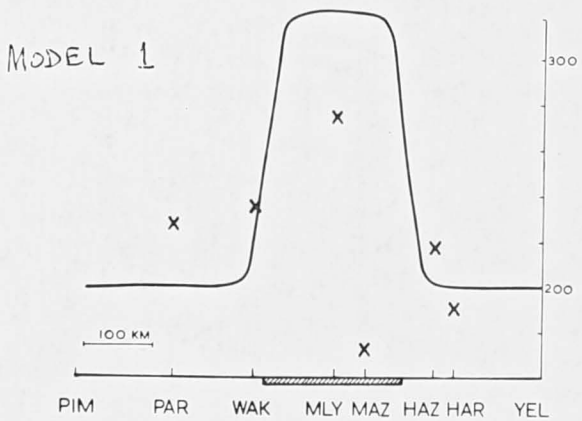

Z - AMPLITUDE

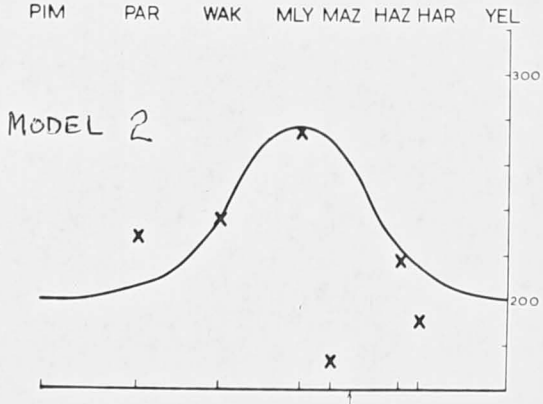

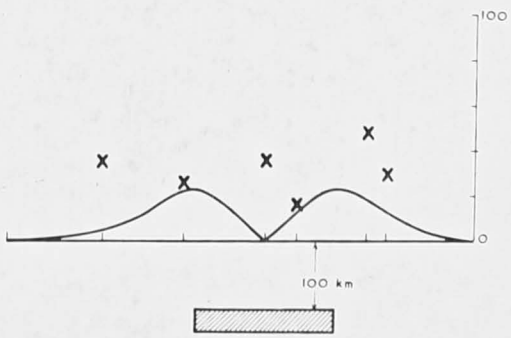

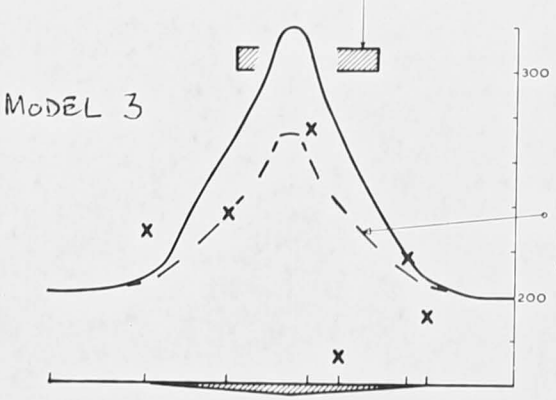

including conductivity increase at 400 km depth

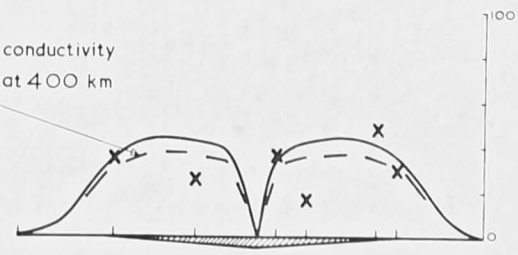

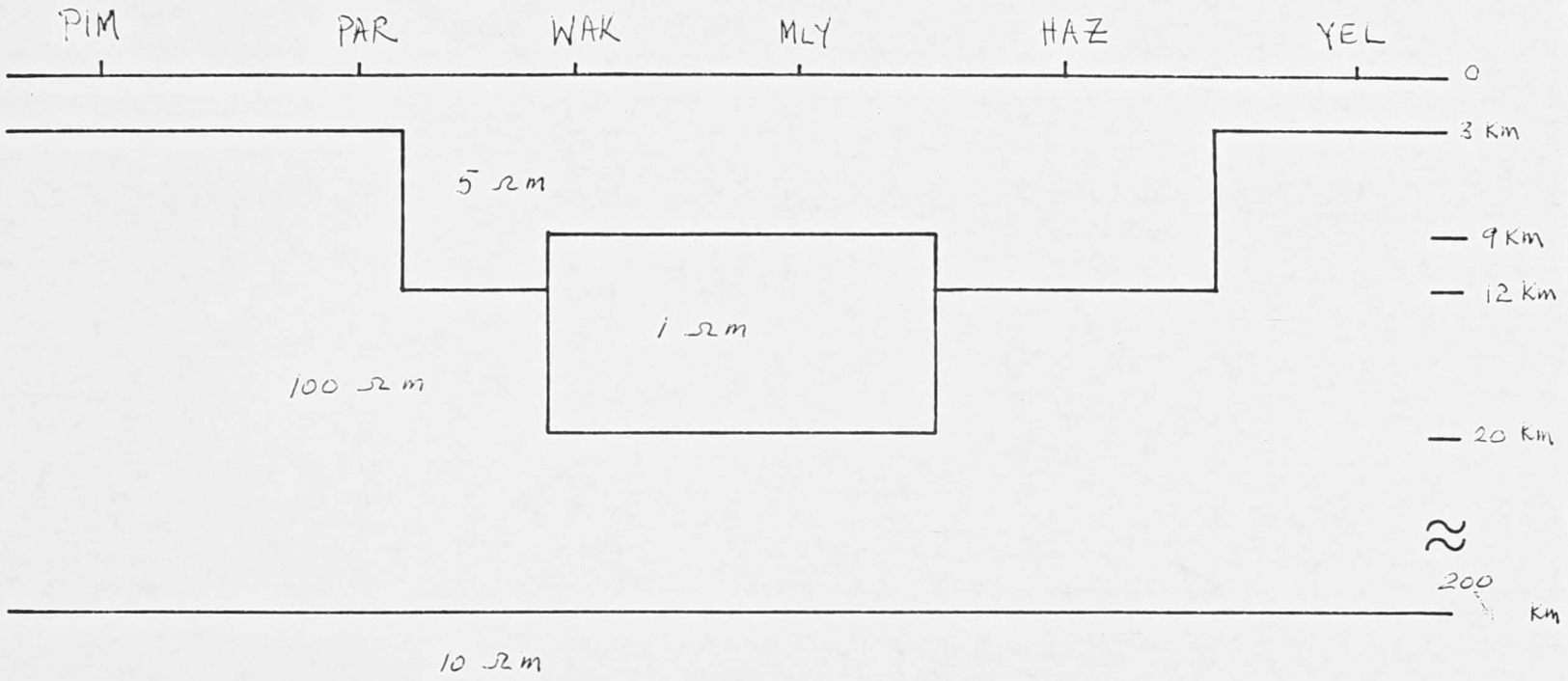
PIM
PAR
WAK
MLY
HAZ
YEL
0
3 Km
9 Km
12 Km
20 Km
≈ 200 Km
5 Ωm
1 Ωm
100 Ωm
10 Ωm

Fig. 8

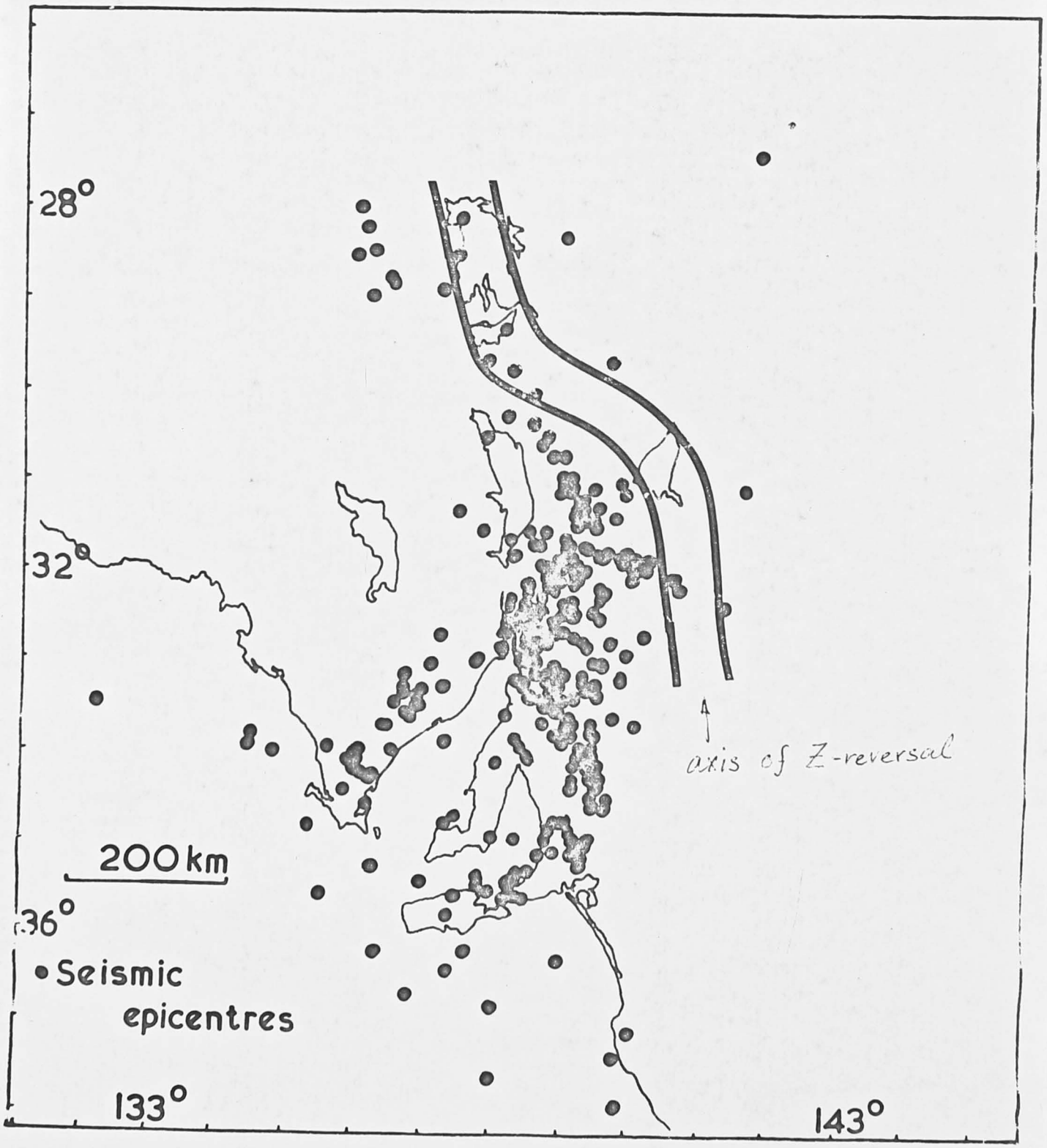

Fig. 9

"A Magnetotelluric Traverse in southern Australia"

H.Y. Tammemagi
F.E.M. Lilley

Dept. of Geophysics and Geochemistry
Australian National University, Canberra

ABSTRACT

Telluric potentials were recorded at nine sites stretching 1000 km from east of Wilcannia (N.S.W.) to west of Coober Pedy (S.A.) in south central Australia. These were combined with data obtained from a simultaneous magnetic variometer study, and analyzed to yield magnetotelluric impedance tensors. The estimation of probable errors for the impedance tensors was an important part of the calculations. Numerical calculations for two-dimensional models showed that the observed data could be explained by a conductive-resistive-conductive layering. The top conductive (10 ohm-m) layer is approximately 5 km deep and the ensuing resistive section (1000 ohm-m) continues to a depth of about 230 km. This is underlain by an indeterminately thick conductive layer. Embedded in this general structure is an extremely good conductor (0.1 ohm-m) which strikes north-south. The detection of this good conductor is the main result of this work. The good conductor lies just east of the Adelaide Geosyncline at a depth of a few kms, and is of minimum thickness 10 km. It is thought to be either directly or indirectly related to the accretion of the eastern portion of the Australian continent onto the stable western Precambrian platform by tectonic processes. The strong anisotropy present in the magnetotelluric data at all sites could not be explained by induction in conductive sediments, and is thought to be caused by local current channelling.

INTRODUCTION

Since its introduction by Cagniard (1953) as a possible geophysical tool, the contributions of the magnetotelluric (M-T) method to the understanding of the earth have been rather indefinite. An early compilation of M-T results by Fournier (1962) showed that not only are the data very scattered, but also the apparent resistivity curves obtained at any one site from orthogonal magnetic and electric components are invariably widely different; that is, anisotropic. Performing a telluric traverse in conjunction with a magnetometer array study in southern Australia provided an excellent opportunity to examine some of these inconsistencies. The Australian inland provides a laboratory generally free of any cultural electromagnetic noise, and there is little topographic variation to perturb the telluric currents. Most important, however, is the opportunity which arises of comparing the electrical conductivity structure derived from the magnetotelluric data with the results obtained independently from the magnetometer array study.

This paper presents the results of the magnetotelluric analysis only. A separate paper is in preparation by Gough et al (1972b), describing the magnetometer array experiment in detail; it has already been mentioned briefly by Gough et al (1972a).

GEOLOGY

The area under study lies across the Adelaide Geosyncline joining the two contrasting regions on either side. To the west lies Precambrian shield and to the east a succession of generally younger rocks; however the zone of demarkation is not clear and occasional Precambrian outcrops have been found to the east. The two regions differ in heat flow, the eastern region having a value generally higher than that of the west (Jaeger, 1970). The travel times of seismic waves also show a difference, being greater to the east (Cleary et al, 1972). The Adelaide Geosyncline, marking the line of division, appears to be the southern extremity of a major crustal feature, the Fitzroy-Spencer fracture zone. Studies of Australian seismicity by Doyle et al (1968) and others have been interpreted in terms of plate tectonics by Cleary and Simpson (1971), who suggest that this fracture zone separates two adjacent crustal blocks. The geosyncline was formed by a great orogeny, in the late Cambrian to Ordovician, of vast accumulated sediments; at present, the area is one of complexity and fracturing, and is a major source of seismicity.

THE EXPERIMENT

The array of twenty-five magnetic variometers was in operation for approximately three months, from mid-September to early December, 1970. By contrast, all telluric observations were made with just three recording units. These were set up at the three eastern-most stations of the line and run simultaneously for one month, then shifted westward to three new localities for the next month, and then finally moved once more. A total of nine stations were thus occupied in three stages by the telluric instruments, and these are shown in Figure 1 together with the sites of the array magnetometers. Table 1 lists the magnetotelluric sites, their code names, and their geographic coordinates, in addition to their dates of operation. The installation and operation of the telluric apparatus was independent of the magnetometer array maintenance.

Three identical telluric recording instruments were especially built for this investigation. Arucomp 4100 recorders (manufactured by Hartmann and Braun) were modified to operate from car batteries for continuous periods of about 10 days. The potential difference, between buried lead plates 500 m apart, was measured with an accuracy of better than 0.5 mv/km. Each instrument recorded two channels: the telluric potentials in the magnetic north and east directions (designated A and B respectively). The potentials were filtered and recorded directly onto 10 day chart paper by ink ribbon, using a dotting interval of 10 seconds. Timing marks were

recorded manually at the start and finish of the chart with the aid of a Bulova Accutron clock, synchronised to radio time signals. The instruments were successfully tested prior to this study and the results have been reported elsewhere (Lilley and Tammemagi, 1972).

The magnetometers were of the type described by Gough and Reitzel (1967). The principle of operation is classical, with magnets suspended on torsion fibres deflecting light beams across photographic film. The three orthogonal magnetic elements, H,D,Z were recorded at 10 sec intervals to an accuracy of better than one gamma (nanoTesla). The instruments were battery powered and ran unattended for periods of three weeks. Hourly timing marks were recorded automatically as deflections in the traces by Bulova Accutron time pieces.

By recording electromagnetic phenomena in the period range of minutes to several hours , it was possible to obtain electrical conductivity information from a few km to a few hundred km depth.

The Impedance Tensor

The impedance tensor, Z_{ij}, is defined by

$$E_1 = Z_{11}H_1 + Z_{12}H_2$$
$$E_2 = Z_{21}H_1 + Z_{22}H_2 \qquad (1)$$

where E_i and H_i denote components of the electric and magnetic field, respectively (Cantwell, 1960). Equation (1) is the mathematical statement that a particular component of the electric field can be induced linearly not only by the magnetic field orthogonal to it, but also by the parallel component. In the case of departure from a layered laterally homogeneous earth, the impedance tensor is a very diagnostic set of parameters. For a two-dimensional earth with the measuring axes aligned parallel and perpendicular to the axis of strike, the impedance tensor becomes

$$Z_{11} = Z_{22} = 0$$
$$Z_{12} \neq Z_{21} \qquad (2)$$

Thus, if a two-dimensional structure is present it should be possible to computationally rotate the impedance tensor, testing whether equation (2) is satisfied for any particular angle of rotation. Usually the diagonal elements Z_{11} and Z_{22} will have minima. These may, however, not be zero, and to determine whether a two-dimensional interpretation is reasonable a skew coefficient can be formed (Swift 1967)

$$\text{skew} = (Z_{11}+Z_{22})/(Z_{12}-Z_{21})$$

The skew is invariant under rotation and approaches zero for a two-dimensional structure.

Analysis and Results

The magnetic film records and the telluric charts were visually inspected, and seven sections were chosen for analysis. These are listed in Table 2 with times in G.M.T. Figure 2 illustrates some of these events. The data were chosen so that each section contained one or more complete transient events, such as sub-storms or bays.

Enlarged Xerox charts were prepared from the chosen magnetic films and these, together with the telluric charts, were digitized at 30 sec intervals. To avoid aliasing problems it was necessary to first smooth the high frequency events manually. The subsequent analyses were performed on an IBM 360/50 computer at the Australian National University Computer Center.

A major feature of the data analysis method is to treat transient events which have been recorded in full. Then any one particular event is independent of those before and after it, and the earlier and later portions of the record may be put equal to zero. The spectrum obtained by Fourier transformation of such a time series is then, in principle, valid for all frequencies. If the event is, for example, a truncated sinusoidal variation, then the sidelobes in the spectrum can be used for analysis as well as the main peak. If there are two such independent events the impedance tensor can be solved using equation (1). Denoting the event numbers by superscripts one obtains

$$Z_{xy} = \begin{vmatrix} H_x^1 & E_x^1 \\ H_x^2 & E_x^2 \end{vmatrix} \Big/ \begin{vmatrix} H_x^1 & H_y^1 \\ H_x^2 & H_y^2 \end{vmatrix} \qquad (3)$$

It is apparent from the denominator that the solution is indeterminate if the magnetic polarizations are not different for the two events.

One advantage of calculating the impedance tensors by this method is that errors can be assigned to the tensor elements in a straight-forward manner. This is a significant step as it allows the reliability of the results to be gauged. Defining a probable error as one which has a 50% probability of being exceeded, it can be shown that the probable error of a Fourier coefficient is $\sqrt{2/n}\,q$ (Whittaker and Robinson, 1946, p.280) where n is the number of data points and q is the probable error in each. It is now straight forward to carry the errors through the calculations in equation (3), using the rule that for addition and subtraction (multiplication and division) the resultant (fractional) probable error is the square root of the sums of the (fractional) probable errors squared , (Bevington, 1969). It is important to note that equation (3) is composed entirely of complex quantities and there are, therefore, a large number of operations involved in computing the impedance tensor. Hence, the probable error accrues rapidly.

Having carried out the error calculations thus far, a further refinement is available in the determination of the tensor value. If several isolated events are considered, say three, pairs can be formed in three ways. For each pair a solution for Z is available via equation (3), and also a probable error can be calculated. In this

case there are three solutions with attendant probable errors and from them a weighted average can be formed (Bevington, 1963, p.70), as follows:

$$\text{weighted average} = \frac{\Sigma(x_i/\sigma_i^2}{\Sigma(1/\sigma_i^2)}$$

$$\text{probable error of weighted average} = 1./\left[\Sigma 1/\sigma_i^2\right]^{\frac{1}{2}},$$

where the x_i are the impedance element values and the σ_i their probable errors.

The sections of data in Table 2 were subdivided into separate transient events. Each datum point in the original time series was assigned a probable error of one gamma or 1 mv/km, as an estimate of the accummulated errors, such as those due to instrument drift, calibration and chart digitization. Linear trends were removed to ensure that no effects of longer period phenomena like the diurnal variation were involved, and then impedance tensors and their probable errors were calculated by the method just described. Figure 3 shows the results for Yelta, and it is seen that at long periods the impedance tensors are stable and have reasonable errors. However, as the periods decrease the fluctuations of the tensor elements increase as do their errors; in fact, at a period of about 500 sec. the probable errors become larger than the values to which they refer. It was decided that a fractional probable error of greater than one was too large to be acceptable, and all such values were subsequently disregarded. This discrimination had the effect of imposing a serious high frequency cut off to the data.

In order to widen the frequency band-width, the original data was searched again for transient events of high frequency content. Trains of micro-pulsations, characteristically of period one to three minutes, were found in bursts throughout the records. These proved to be ideal; the ones chosen were digitized manually and analysed by the method described above.

To obtain further statistical smoothing of the results, the impedance tensor element values were band-width averaged.

Skew coefficients were calculated, and as an example those for Yelta as shown in Figure 4. There are no strict rules for the interpretation of skew coefficients, but values of 0.2 or less as for the long-period data at Yelta would generally be taken to indicate two-dimensional structure, (Swift 1967, Vozoff 1972). All the stations except Mulyungarie yielded similarly small skew values, indicating two-dimensionality.

In Figure 5 the impendance tensors for the different stations are presented as polar plots, for a period of 2270 sec. The radial distance and the azimuth represent the absolute value of the tensor element and the rotation angle respectively, (see, for example, Berdichevskiy et al, 1970). The polar plots show a distinct variation in impedance magnitude across the traverse and two-dimensionality of structure is indicated by the pattern of four distinct lobes for Z_{xx}, together with the two-lobed pattern for Z_{xy}.

Finally, apparent resistivities for the principal directions were calculated from the equation

$$\rho_a = 0.2T\,|Z|^2$$

where ρ_a is the apparent resistivity in ohm-m, T the period in sec, and Z is an off-diagonal element of the rotated impedance tensor. The apparent resistivities, together with their probable error bars, are shown in Figure 6.

Interpretation

Several important facts are immediately evident from inspection of the apparent resistivity curves (Figure 6). Taking each station individually, in every case the ρ_{yx} curve is different from the ρ_{xy} curve, in many instances by an order of magnitude. The two-dimensionality of this effect has already been noted, though it will be shown later that this anisotropy is more local than regional, and is, in fact, a severe obstacle to the accurate interpretation of the data.

The dominant result of the experiment, however, stands out clearly above anisotropy effects, and is expressed by the very low apparent resistivities recorded at Waukaringa and Mulyungarie. This is also indicated in Figure 2 by the high attenuation of the natural telluric signals at these sites relative to the stations on either side. The presence of a region of very high electrical conductivity has evidently been detected, and the further delineation of this good conductor is an interpretation task of high importance.

To commence the interpretation, an assumption was made that the electrical conductivity structure beneath Waukaringa and Mulyungarie is two-dimensional, so that a line from Pimba to Yelta direct would be at right angles to the strike. This assumption is supported by the tectonic lineations of the Adelaide geosyncline, and also, quite independently, by the magnetometer array data of Gough et al (1972a). Computations of particular two-dimensional

models were then carried out, following the methods of Jones and Price (1970) and, in particular, using the programs of Jones and Pascoe (1971) and Pascoe and Jones (1972). Some twenty models were investigated, each one at several different frequencies. On the basis of certain initial assumptions, the final model was determined to within quite useful limits. An initial assumption was that an overburden of resistivity 10 ohm-m, 5 km deep, overlaid the whole region. The resistivity of this overburden was taken from the values of the apparent resistivity at the lowest periods of Figure 6, and is reasonable for the surface of inland Australia, which in places is covered with salt lakes, and is generally quite conductive. The depth of 5 km was taken from an estimate of the depth of sediment cover in the Adelaide Geosyncline (Stewart and Mount, 1972); it may well be an overestimate for the overburden away from the synclinal area, but this is not likely to seriously affect the general features of the model.

The good conductor, modelled to lie between Waukaringa and Mulyungarie as shown schematically in Figure 7, must have a resistivity as low as 0.1 ohm-m, and for this resistivity it must have a minimum thickness of 10 km; its maximum possible thickness is undetermined. The present data allow the uppermost surface of the good conductor to be arbitrarily near the surface of the ground; on the other hand it cannot be deeper than 10 km. The width of this feature is uncertain, but it must extend past Mulyungarie to the east and Waukaringa to the west. Modelling the good conductor against background resistivities of 100 ohm-m and 1000 ohm-m shows that the latter model (see Figure 7) provides a slightly better fit. Theoretical apparent

resistivity curves for this model are shown superimposed on the data of Figure 6. The theoretical ρ_{xy} and ρ_{yx} curves are almost identical and only the former is illustrated. The smoothing effect of the uniform overburden no doubt plays a major role in this effect. This is an important result, for if the theoretical ρ_{xy} and ρ_{yx} curves are almost identical then the observed anisotropy is not caused by the two-dimensionality of this model, and remains to be explained. At this stage, the interpretation could proceed by assuming a layered earth under each station and then fitting model curves (eg. Srivastava, 1967) separately to each site.

Another feature of the apparent resistivity curves is their "turn over" at long periods. If this is interpreted in terms of a highly conducting, lower region of resistivity 10 ohm-m, then the depth at which this region is encountered must be between 200 and 260 km.

Some discussion may now be given regarding the anisotropy, mentioned above for the data in hand, and in fact found almost universally in magnetotelluric experiments.

Because the principal axes of the impedance tensors at the different sites all showed an approximate north-south trend (Figure 5), the anisotropy was originally thought to be the effect of a large, near-surface conductor to the north of the traverse (perhaps the Great Artesian Basin), superimposed upon the effect of the main model already described. The 1000 foot depth contour of the Great Artesian Basin is marked on Figure 5, and it can be seen to be generally orthogonal to the principal axes of the impedance tensors. Figure 8 shows the model

examined to test this possibility: a sharp change occurring in the resistivity of surface sediments at a vertical contact. Also shown in Figure 8 is the anisotropy which results, plotted as distance from the contact on the more resistive side. It can be seen that only within 25 km of the contact do the maximum and minimum apparent resistivity curves separate by an order of magnitude. This appears to render untenable the hypothesis that the observed anisotropy is caused by the Great Artesian Basin: for most observing sites are further than 25 km away (see Figure 5).

It thus appears that the observed M-T anisotropy cannot reasonably be explained by induction on a regional scale; a likely alternative is, therefore, that it is caused by local channelling of telluric currents which are induced elsewhere, as in the cases studied by Dyck and Garland (1969), and Lilley and Tammemagi (1972). If this is so, then in the present case, the current channelling mechanism has been particularly deceptive, because the resulting skew coefficients and rotation angles are indistinguishable from those caused by induction in a two-dimensional structure. The common occurrence of such anisotropy remains one of the greatest disadvantages of the magnetotelluric method.

Discussion

The major feature of the model is the large conductive block below Mulyungarie and Waukaringa. Perhaps surprisingly this is located just to the east of the Flinders Ranges and not under them. It is of great interest to compare this result with the interpretation of the magnetometer array data, and model studies have been commenced for this specific purpose, (Lilley et al, in preparation); the preliminary results substantiate the presence and location of this conductive feature. The discovery of such a large volume of highly conducting rock in the crust is quite remarkable. As a case history it may be compared to the magnetotelluric work of Vozoff and Swift (1968), which described sediments of high conductivity in the North German basin: other major crustal conductors are mentioned by Garland (1971).

A tentative geological interpretation of this result is now presented. Dewey and Bird (1970) explain the formation of geosynclines in terms of miogeoclinal and eugeoclinal couplets, formed by the growth of continents by tectonic global processes. Oversby (1971) has concluded from geologic evidence that eastern Australia was formed by the interaction of the continental block with island arcs and trenches. Thus, the Adelaide Geosyncline would be the remnant of one couplet, and the other couplet would lie buried to the east, under Mulyungarie and Waukaringa. Whether the eastern material is itself more conductive or whether it is structurally weaker, resulting in greater

fracture zones and higher porosity, and hence higher conductivity, is not known. There is the clear possibility that the sediments may contain a great deal of saline water.

It is also of interest to offer an interpretation for the deep zone of high conductivity commencing at a depth of about 230 km. The upper mantle is thought to be composed of peridotite (Ringwood 1969), the most conductive constituent of which is olivine, and the exponential decrease of olivine resistivity with temperature could provide an explanation. Combining the temperature-depth profile of MacDonald (1965) with the compilation of experimental conductivity-temperature results for 10% fayalite olivine, (Duba and Lilley, submitted 1972), it is seen that by a depth of order 150 km and deeper the resistivity of olivine might be expected to decrease to about 10 ohm-m. The proposed model is in reasonable agreement with this result.

In summary, the conductivity near the surface is controlled by porosity and water content rather than by petrologic composition. As depth and pressure increase the porosity is reduced and the rocks become resistive; ultimately the temperature-dependent semi-conduction mechanisms of olivine become dominant, and the rocks become increasingly conductive. Thus an overall conductive, resistive, conductive layering results.

Acknowledgements

Above all else, we are indebted to Professor D.I. Gough, who was leader of the project which supplied the magnetometer data, and who provided us with much stimulating discussion and instruction. We are grateful to the many people who assisted us in the field, and particularly we thank the station owners and managers at our sites; we much appreciated the generous hospitality of the Australian outback. The cooperation of the Land Research Unit of the C.S.I.R.O. and the use of their digitizer is appreciated. The authors enjoyed fruitful discussions with Professor E.J. Hannan, Dr. J.R. Cleary, Dr. R.A. Crawford, Dr. A.G. Duba and Mr. D.J. Bennett. One of us (H.Y.T.) was supported by an A.N.U. Research Scholarship.

References

Berdichevskiy, M.N., Dubrovskiy, K.I., Soloklov, V.V., and Faynberg, E.B. 1970, Geoelectric Characteristics of the Earth's Crust and Upper Mantle in Turkmenia: Izv., Earth Physics, v. 11, p. 86-91

Bevington, P.R., 1969, Data Reduction and Error Analysis for Physical Sciences: McGraw-Hill Pub. Co.

Cagniard, L., 1953, Basic Theory of the Magnetotelluric Method of Geophysical Prospecting: Geophysics, v.18, p. 605-635.

Cantwell, T., 1960, Detection and Analysis of low frequency magnetotelluric signals: Ph.D. thesis, Dept.of Geology and Geophysics, Massachusetts Institute of Technology.

Cleary, J.R., and Simpson, D.W., 1971, Seismotectonics of the Australian Continent: Nature, v. 230, p. 239-241.

Cleary, J.R., Simpson, D.W., and Muirhead, K.J., 1972, Variations in Australian Upper Mantle Structure from Observations of the Cannikin Explosion: Nature Phys. Sci., v. 236, p. 111-112.

Dewey, J.F., and Bird, J.M., 1970, Mountain Belts and the new Global Tectonics: J.G.R., v.75, p. 2625-2647.

Doyle, H.A., Everingham, I.B., and Sutton, D.J., 1968, Seismicity of the Australian Continent: J. Geol. Soc. Austral., v. 15, p. 295-312.

Duba, A., and Lilley, F.E.M., submitted 1972 to J.G.R., The effect of an ocean ridge model on geomagnetic variations.

Dyck, A.V., and Garland, G.D., 1969, A Conductivity model for certain features of the Alert anomaly in Geomagnetic Variations: Can. J. Earth Sci., v. 6, p. 513-516.

Fournier, H., 1962, Rev. Assoc. Ing. Gand (Mons): v. 10 p. 9-16.

Garland, G.D., 1971, Electrical conductivity anomalies - mantle or crust? : Comments on Earth Sciences, Geophysics, v.1, p. 167-172.

Gough, D.I., and Reitzel, J.S. 1967, A portable three-component magnetic variometer: J. Geomagn. Geoelec., v. 19, p, 203-215.

Gough D.I., Lilley F.E.M., and McElhinny M.W., 1972a, A polarization-sensitive magnetic variation anomaly in South Australia : Nature, submitted.

Gough, D.I., McElhinny M.W., and Lilley F.E.M. 1972b, in preparation.

Jaeger, J.C., 1970, Heat Flow and Radioactivity in Australia: Earth Planet. Sci. Letters, v. 8, p. 285-292.

Jones, F.W., and Price, A.T., 1970, The perturbations of Alternating Geomagnetic Fields by Conductivity Anomalies: Geophys. J.R. astr. Soc., v. 20, p.317-334.

Jones, F.W., and Pascoe, L.J., 1971, A General Computer Program to Determine the Perturbation of Alternating Electric Currents in a Two-dimensional Model of a Region of Uniform Conductivity with an Embedded Inhomogeneity: Geophys. J.R. astr. Soc., v. 23, p.3-30.

Lilley, F.E.M., and Tammemagi, H.Y., 1972, Telluric Potentials Recorded Simultaneously at three sites near Canberra, A.C.T.(Aust): Geoexploration v. 10, p. 115-120.

Lilley, F.E.M., Gough D.I., Tammemagi, H.Y., in preparation

MacDonald, G.J.F., 1965, Geophysical Deducations from observations of Heat Flow: A.G.U. Monograph 8, ed. W.H.K. Lee.

Oversby, B., 1971, Palaeozoic Plate Tectonics in the Southern Tasman Geosyncline: Nature Phys. Sci., v. 234, p. 45-47.

Pascoe, L.J., and Jones, F.W., 1972, Boundary conditions and calculation of surface values for the general two-dimensional electromagnetic induction problem: Geophys. J.R. astr. Soc., in press.

Ringwood, A.E., 1969, Composition and Evolution of the Upper Mantle: A.G.U. monograph 13, ed. P.J. Hart, p. 1-17.

S rivastava, S.P., 1967, Magnetotelluric two and three layer master curves: Publ. Dom. Obs., Ottawa, 35, No. 7.

Stewart, I.C.F., and Mount T.J., 1972, Earthquake Mechanisms in South Australia in Relation to Plate Tectonics: J. Geol. Soc. Austral., in press.

Swift, C.M. Jr., 1967, A Magnetotelluric Investigation of an Electrical Conductivity Anomaly in the South-western United States: unpublished Ph.D. thesis, Dept. of Geology and Geophysics, M.I.T. Cambridge, Mass.

Vozoff, K., 1972, The magnetotelluric method in the exploration of sedimentary basins: Geophysics, v. 37, p. 98-141.

Vozoff, K., and Swift, C.M. Jr., 1968, Magneto-telluric measurements in the North German Basin: Geophysical Prospecting, v. 16, p. 454-473.

Whittaker, E.T., and Robinson, G., 1946, The Calculus of Observations: Blackie Ltd., London.

Fig. 1. The geographic location of the M-T traverse in Southern Australia. Both telluric and magnetic data were obtained at the sites marked by solid circles, magnetic data only at open circles.

Fig. 2. Simultaneous telluric and magnetic recordings in three stages across the array. (H-magnetic north, D-magnetic east, A-telluric north, B-telluric east). The figures in the center represent event numbers (see Table 2).

Fig. 3. The impedance tensor element, $|Z_{xy}|$, for Yelta and its error. The solid squares represent the absolute value of the impedance tensor and the hollow squares are the errors. The units of the impedance tensor are (mv/km/gamma).

Fig. 4. Bottom: Skew coefficient at Yelta as a function of frequency.

Top: Rotation angle at Yelta plotted against frequency.

Fig. 5. Polar plots of the impedance tensors at a period of 2270 sec, with the 1000 foot depth contour of the Great Artesian Basin.

Fig. 6. Apparent resistivities calculated from impedance tensors which have been rotated into principal axes. The superimposed solid curves represent the theoretical ρ_{xy} curve for the model of "best" fit. Solid squares represent ρ_{yx}, open triangles ρ_{xy}.

Fig. 7. A cross-section of the model (not to scale) which best fits the data.

Fig. 8. Anisotropy as a function of distance, as caused by the contact with the conductive sediments of the Great Artesian Basin. The graph is drawn at a period of 2000 seconds for the positive side of the contact.

TABLE I

Yelta	Yel	31°56'S ,	143°39'E	Sept. 11 - Oct. 6, 1970
Hazelvale	Haz	31°46'S ,	142°16½'E	Sept. 11 - Oct. 6, 1971
Mulyungarie	Mly	31°33'S,	140°47½'E	Sept. 9 - Oct. 7, 1970
Waukaringa (Melton)	Wak	32°20'S,	139°21'E	Oct. 8 - Nov. 3, 1970
Partacoona	Par	32°0½'S,	138°9½'E	Oct. 9 - Nov. 3, 1970
Pimba (Woomera)	Pim	31°8'S,	136°48½'E	Oct.10 - Nov. 4, 1970
Billa Kalina	Bil	29°55'S,	136°11½'E	Nov. 5 - Dec. 4, 1970
Ingomar	Ing	29°38½'S,	134°48' E	Nov. 6 - Dec. 3, 1970
Tallaringa	Tal	28°56½'S,	133°59½'E	Nov. 7 - Dec 2, 1970

TABLE 2

Event No.	1	Oct. 4, 1970	09:30 - 15:30
	2	Sept. 13	03:00 - 17:00
	3	Sept. 14	10:30 - 16:30
	4	Oct. 16	09:00 - 22:00
	5	Oct. 23	12:30 - 18:00
	6	Nov. 7	00:00 - 16:00
	7	Nov.15-16	23:00 - 02:00

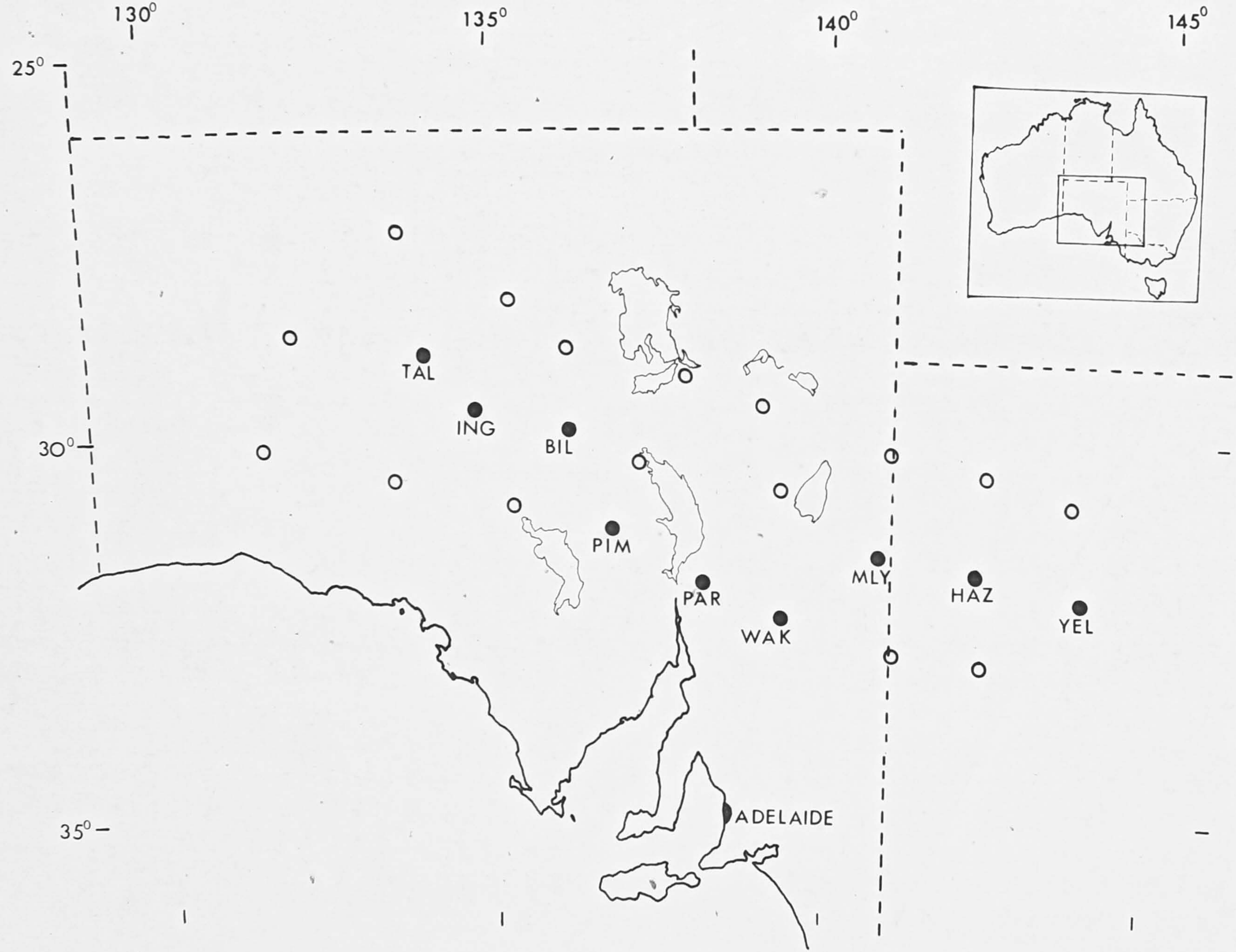

Figure 1 Tammemagi & Lilley

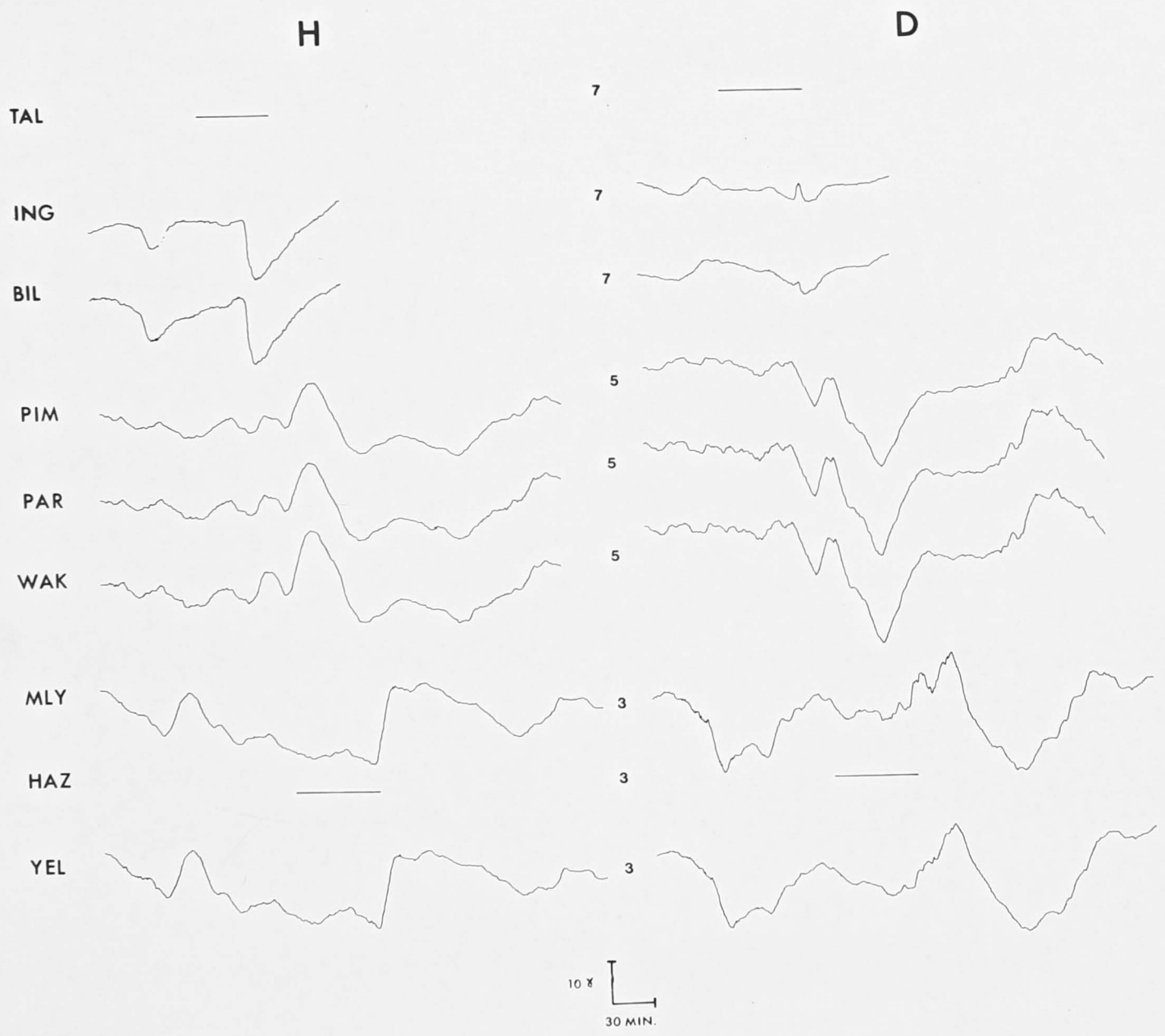
H
D
TAL
ING
BIL
PIM
PAR
WAK
MLY
HAZ
YEL
7
7
7
5
5
5
3
3
3
10 %
30 MIN.

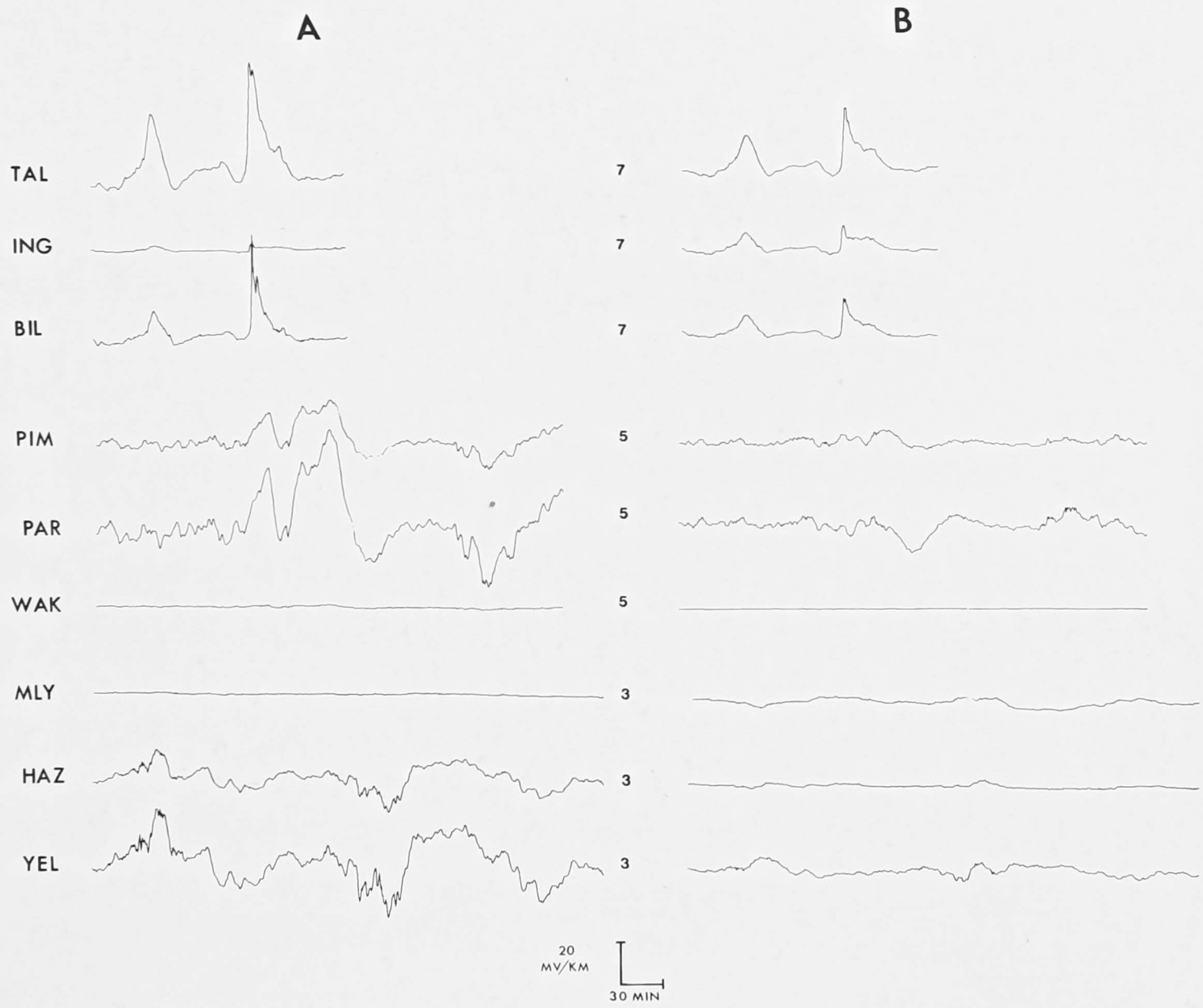
A
B
TAL
ING
BIL
PIM
PAR
WAK
MLY
HAZ
YEL
7
7
7
5
5
5
3
3
3
20
MV/KM
30 MIN

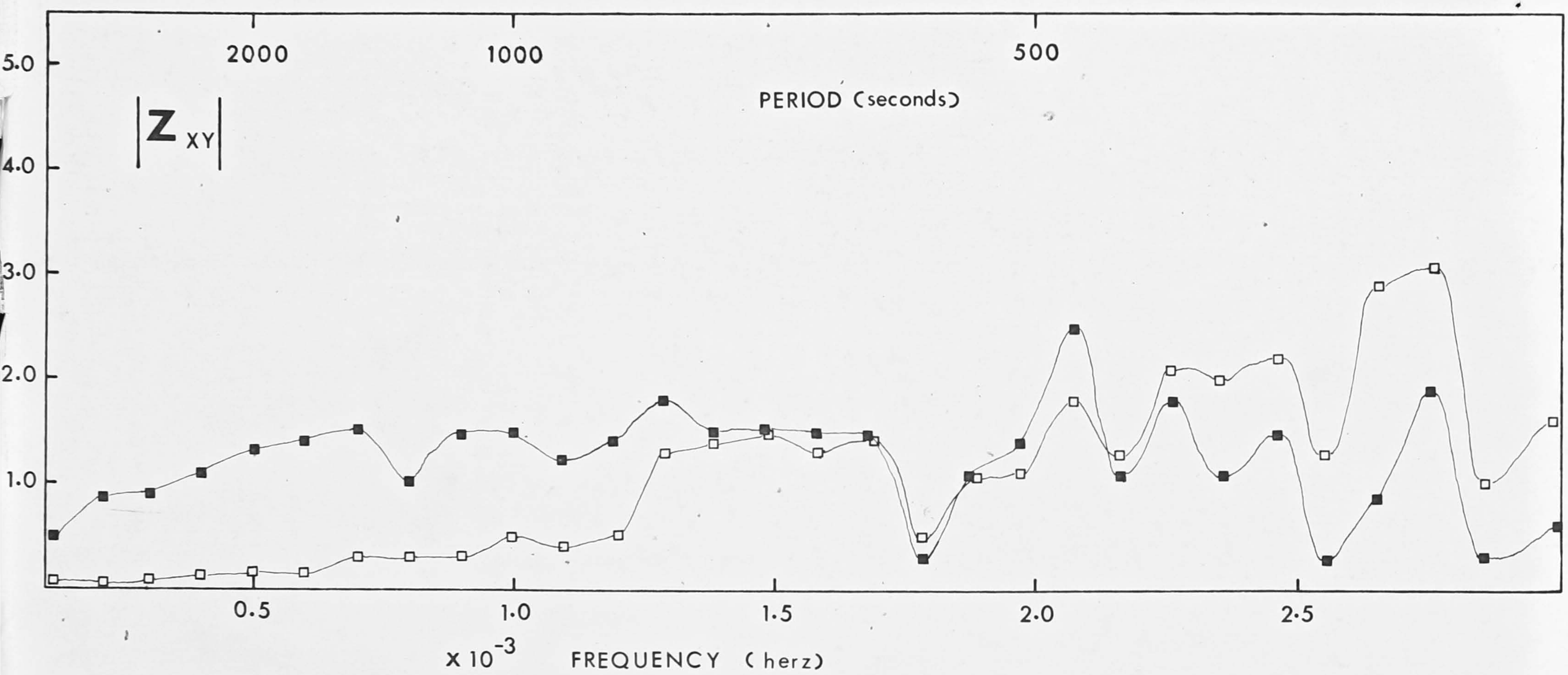
PERIOD (seconds)
2000
1000
500
|Z XY|
5.0
4.0
3.0
2.0
1.0
0.5
1·0
1·5
2·0
2·5
x 10⁻³ FREQUENCY (herz)

Figure 3. [illegible]

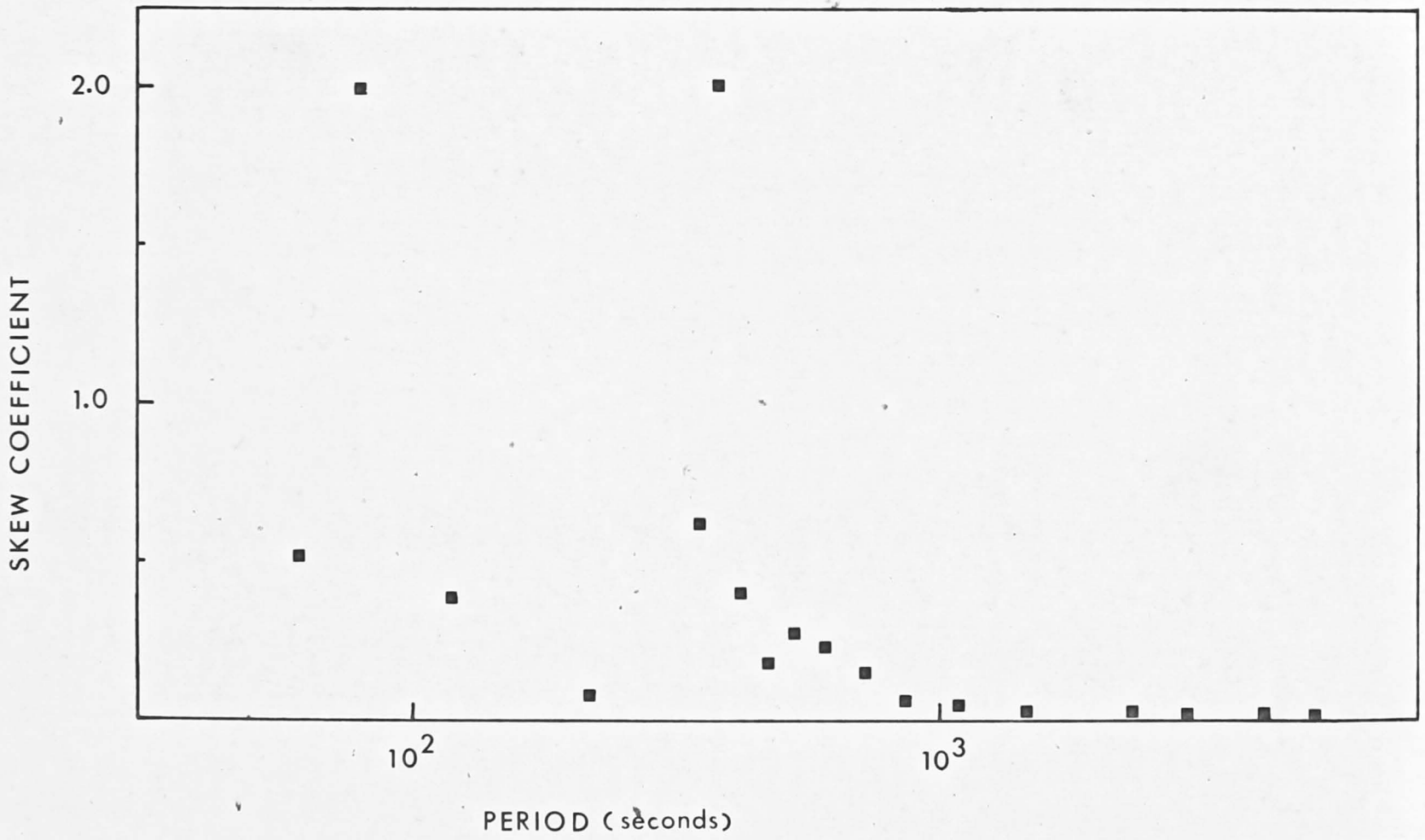
2.0
1.0
SKEW COEFFICIENT
10^2
10^3
PERIOD (seconds)

1000'
TAL
ING
BIL
1000'
PIM
PAR
WAK
MLY
HAZ
YEL
Z_{XY}
Z_{XX}
200 km.
1 Z unit

APPARENT RESISTIVITY (Ω-m)
TAL
ING
BIL
PIM
PAR
WAK
MLY
HAZ
YEL
PERIOD (seconds)

Tammemagi & Lilley Figure 7

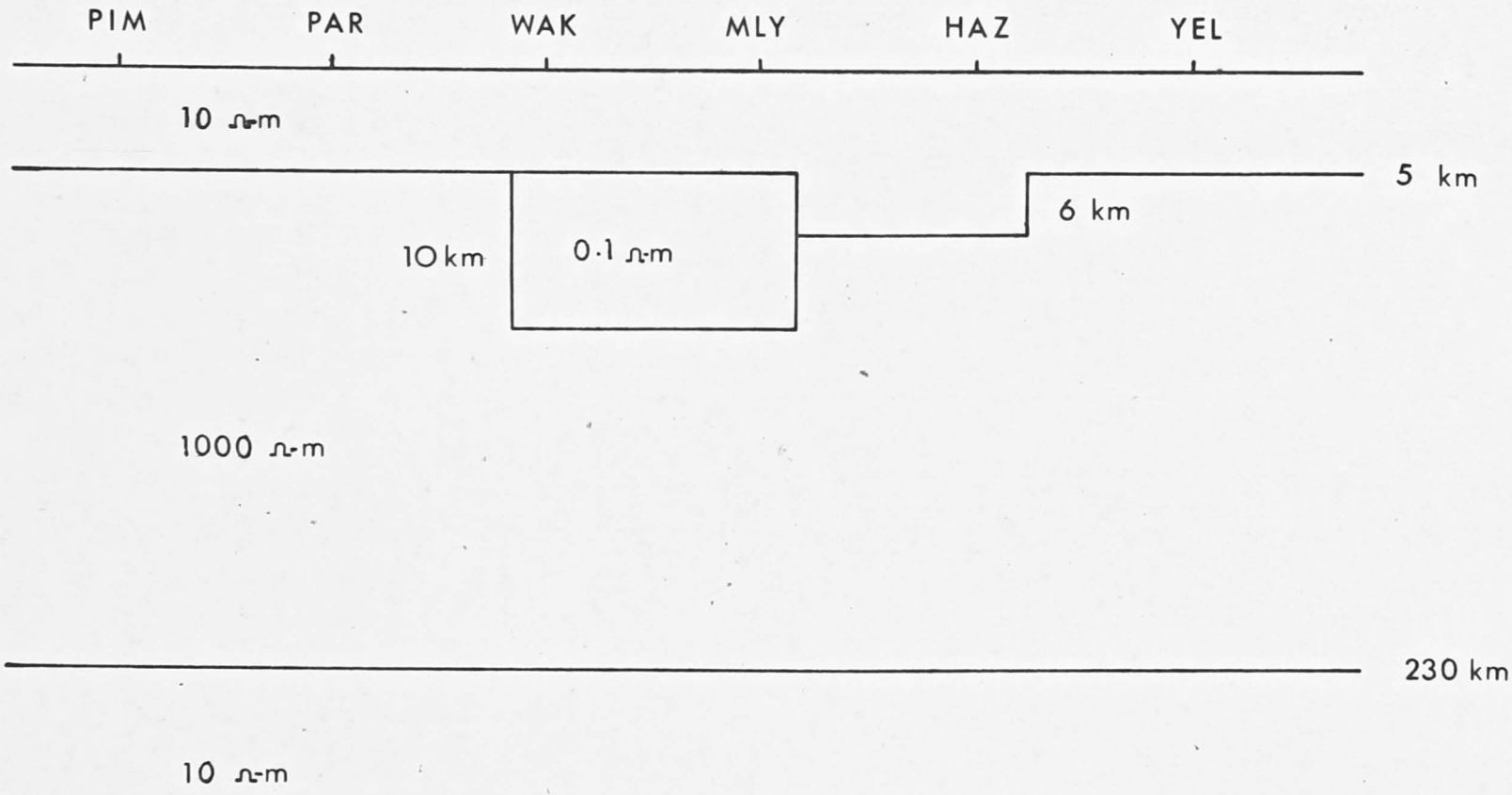

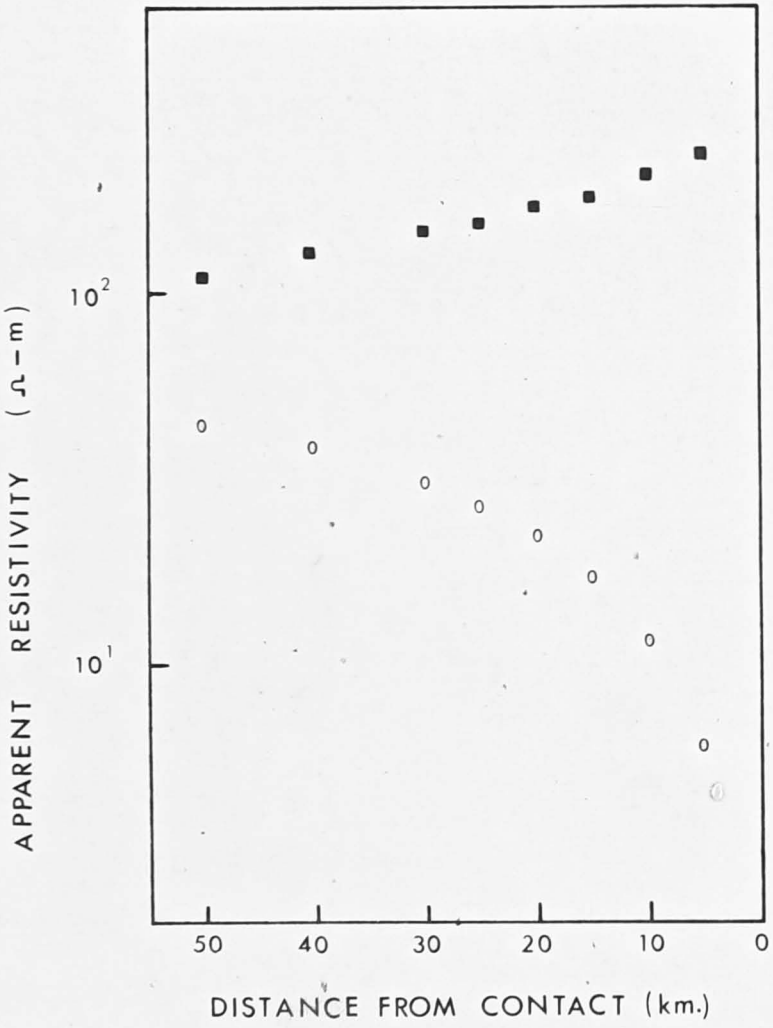
APPARENT RESISTIVITY (Ω-m)
10^2
10^1
50
40
30
20
10
0
DISTANCE FROM CONTACT (km.)

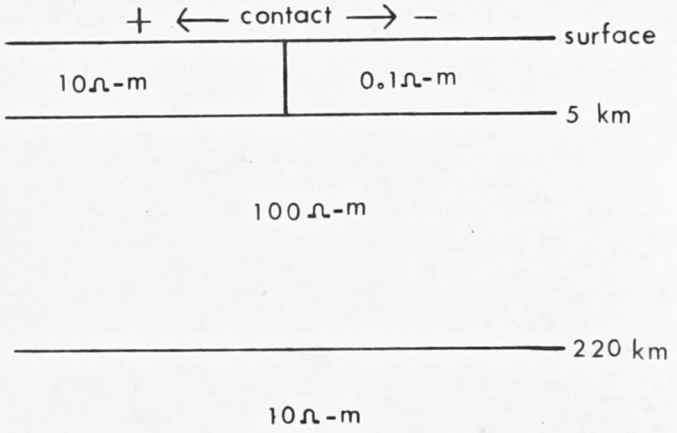
+ ⟵ contact ⟶ −
surface
10Ω-m
0.1Ω-m
5 km
100Ω-m
220 km
10Ω-m